Dissociation of Methylammonium Cations in Hybrid Organic-Inorganic Perovskite Solar Cells: Supporting Information

Weidong Xu, Lijia Liu,* Linju Yang, Pengfei Shen, Baoquan Sun, and John A. McLeod*

Institute of Functional Nano and Soft Materials (FUNSOM) ,Jiangsu Key Laboratory for Carbon-Based Functional Materials & Devices, Soochow University, Suzhou, Jiangsu, 215123 China

E-mail: ljliu@suda.edu.cn; jmcleod@suda.edu.cn

Abstract

Details of the sample preparation and characterization, of the X-ray spectroscopy measurements, and the density functional theory calculations are given here.

Sample Preparation and Characterization Methods

Perovskite films were prepared by first spin-coating PEDOT:PSS (CLEVIOS AL 4083) at 4000 rpm for 40 s on a clean ITO coated glass substrate (sheet resistance 20 $\Omega{\cdot}\mathrm{cm}^2$), then baked at 140 °C for 15 min. The substrates were then transferred to a glove box and spin-coated with a 40 %wt $CH_3NH_3PbI_{3-x}Cl_x$ precursor solution ($PbCl_2$ mixed with CH_3NH_3I with a molar ratio of 1:3 in dimethylformamide (DMF)) at 3000 rpm for 40 s. The perovskite

*To whom correspondence should be addressed

films were then baked on a hot plate at 95 °C for 20 min., allowing the colour of the perovskite films to turn from yellow to dark brown.

Scanning electron microscopy (SEM) measurements were performed on select films, while other select films were sealed as-prepared under nitrogen and transported to the Canadian Lightsource for X-ray spectroscopy measurements. All X-ray spectroscopy measurements were performed under ultra-high vacuum conditions (pressures at 10^{-7} torr or lower). High-resolution X-ray absorption (XA) measurements at the carbon and nitrogen K were performed at the SGM beamline[1] in bulk-sensitive partial fluorescence mode, while high-resolution X-ray emission (XE) measurements at the carbon and nitrogen K-edges were performed at the REIXS beamline. Lower-resolution XA measurements were also performed at REIXS to ensure accurate energy calibration with the measurements from SGM. Measurements were performed at several locations on the samples; these measurements were all self-consistent. X-ray diffraction (XRD) measurements (PANalytical, by Empyrean) were performed on films that had an additional layer of PMMA (10 mg/ml in chlorobenzene) spin-coated at 3000 rpm for 40 s in a glove box, this was to help protect the films from the atmosphere during the ambient XRD measurements.

For the ^{1}H nuclear magnetic resonant (NMR) measurements we first scraped pristine $MAPbI_3$ films from their substrates and dissolved them in DMSO-d6. MAI and MI powders were also dissolved in DMSO-d6 as reference compounds. ^{1}H NMR spectroscopy was performed using a BRUKER AVANCE III 400 MHz spectrometer at room temperature. The ^{1}H chemical shifts are referenced to the DMSO-d6 residual solvent signal at 2.50 ppm. For comparing the stoichiometries of the NH_3 and CH_3 groups, the integration range was chosen as 3 full-widths at half-maximum (FWHM) on either side of the spectral peak; increasing or decreasing the range by an additional FWHM changes the ratio of the areas by less than 2%.

X-ray photoelectron spectroscopy (XPS) measurements were carried out in a SPECS ultrahigh vacuum photoelectron spectroscopy system using a monochromatized Al Kα source

(1486.7 eV). The base pressure was 10^{-10} mbar during the measurements.

Solar cells were fabricated from 20 of the remaining films. A PCBM solution (30 mg/ml in chlorobenzene) was spin-coated on top of the perovskite at 2000 rpm for 40 s, followed by spin-coating a colloidal ZnO nanocrystal solution (8 mg/ml in ethanol) at 3000 rpm for 40 s. Finally, the as-prepared devices were covered by shadow masks and an aluminum electrode (120 nm thick) was deposited by thermal evaporation (Mini SPECTRO, Kurt J. Lesker). The device area was 0.0725 cm^2 as determined by the shadow masks. The device current density-voltage curves were measured under an AM 1.5G 100 MW/cm^2 solar spectrum irradiation source provided by a Newport 94023A solar simulator.

Device Characterization

Additional SEM images at various magnifications are shown in Fig. S1.

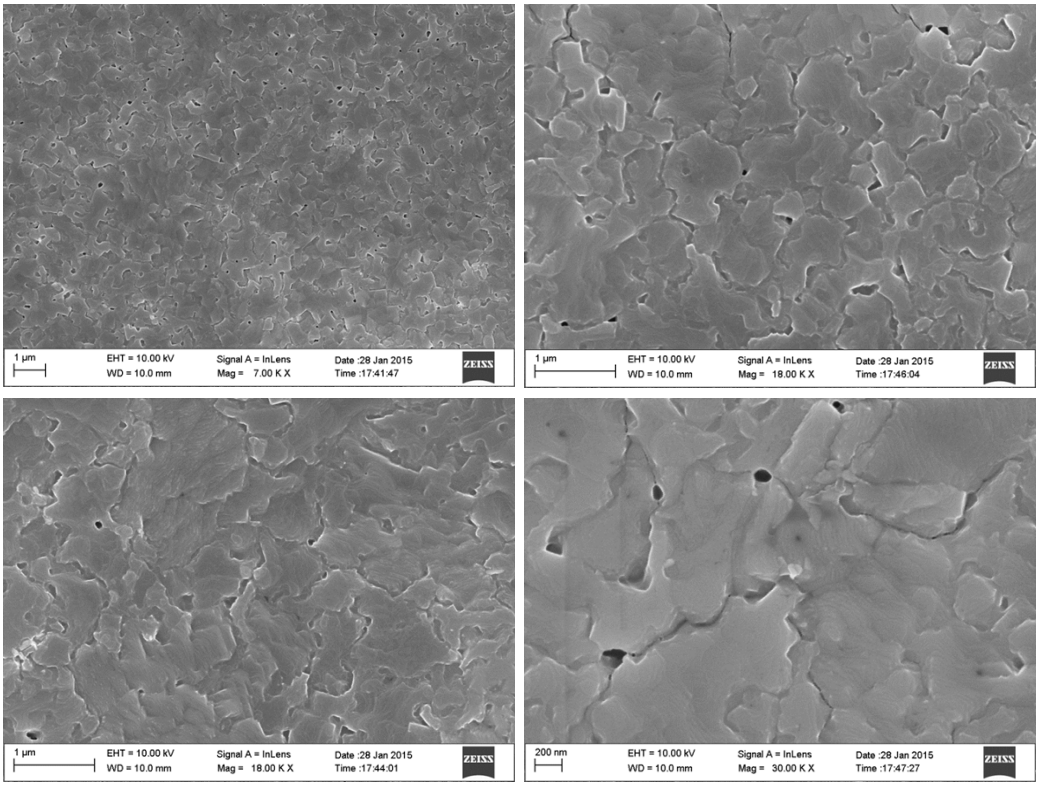

Figure S1: Additional SEM images.

The current density-voltage curves were measured with a scan rate of 1.05 V/s, with no dwell times. No preconditioning protocol was used. The external quantum efficiency and integrated response of a standard reference spectrum are shown in Fig. S2.

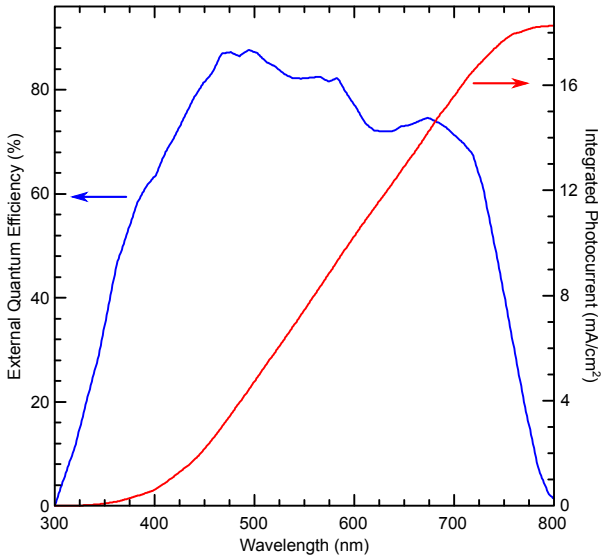

Figure S2: The external quantum efficiency and integrated response of a photovoltaic device.

Density Functional Theory Calculations

All density functional theory (DFT) calculations were performed with WIEN2k[2] using the Perdew-Burke-Ernzerhof exchange-correlation functional,[3] which has been found to accurately reproduce the electronic structure of these perovskites due to a fortuitous error cancellation.[4] The product of the smallest muffin-tin radii, R_{MT}^{min} and the largest planewave K^{max} was set to 3.0, and 125 k-points were used. Since the smallest R_{MT} was 0.68 bohr for hydrogen, the K^{max} for these systems is actually larger than it would be for most inorganic semiconductors (Si, TiO_2, ZnO, etc. using the typical value of $R_{MT}^{min}K^{max} = 7$, as in those cases generally $R_{MT}^{min} > 1.6$ bohr.

A single pseudo-cubic perovskite cell with the appropriate organic molecule was used for to simulate the X-ray spectra. The atomic coordinates of all atoms was fully relaxed using the MSR1a optimization method.[5] The spectra were obtained from the electronic structure using the XSPEC program to calculate the transition matrix elements.[6] The reported XAS spectra were simulated using a full core-hole in the $1s$ orbital of the absorbing atom (C or N, as appropriate).

Using $MAPbI_3$ as a test case, increasing $R_{MT}^{min}K^{max}$ to 3.5 and increasing the number

of k-points to 1000 decreased the total energy of the system by only 0.5 eV/unit cell, and descreased the Fermi level by only 0.1 eV. More importantly for our purposes, increasing $R_{MT}^{min}K^{max}$ and using a denser k-grid changes the carbon and nitrogen $1s$ core levels by 0.1 eV or less, which is smaller than the energy resolution of our measurements. The carbon and nitrogen $2p$ densities of states (DOS) likewise were essentially the same for these calculations. Since we are not interested in calculation formation enthalpies or determining the electronic structure near the valence band maximum or conduction band minimum, we consider $R_{MT}^{min}K^{max} = 3.0$ and a 125 k-point grid to be sufficient for our purposes.

In all cases the X-ray absorption (XA) was simulated using a single core hole in the carbon and nitrogen $1s$ state, as appropriate of a single unit cell. Since DFT is inherently periodic, this puts a separation of just over 6 Åbetween adjacent core holes. In the actual measurements, the distance between core holes is considerably greater. However since the organic molecules have almost negligible hybridization with the much nearer Pb-I lattice, we consider this distance sufficient to prevent any significant interaction between core holes. The fact that our simulations are in good agreement with our measurements verifies this assumption.

The simulated X-ray emission (XE) and XA spectra were aligned with the measured spectra by adding the difference between the Fermi energy of the ground state or core hole-perturbed system (for XE and XA, respectively) and the calculated ground state eigenvalues of the carbon and nitrogen $1s$ level, as appropriate. This process allows our different simulations to be directly compared on the same energy scale. DFT underestimates the core state energies, so the simulated spectra had to be shifted by a further 16.8 eV for the carbon K XE and XA, and 21.2 eV for the nitrogen K XE and XA.

We note that the assumption that DFT will underestimate the core state energies all by the same fixed amount is not necessarily true; it is possible that different model compounds may require slightly different energy shifts. We do expect the differences to be on the order of a few 100 meV or less, however because of this possibility we have avoided trying to

quantify the presence of other organic components by fitting the measured spectra with the simulated spectra, since the fit would be extremely sensitive to small energy shifts in the simulated spectra.

For reference, the DOS of $MAPbI_3$ is shown in Fig. S3, our results are essentially the same as those found in the literature.

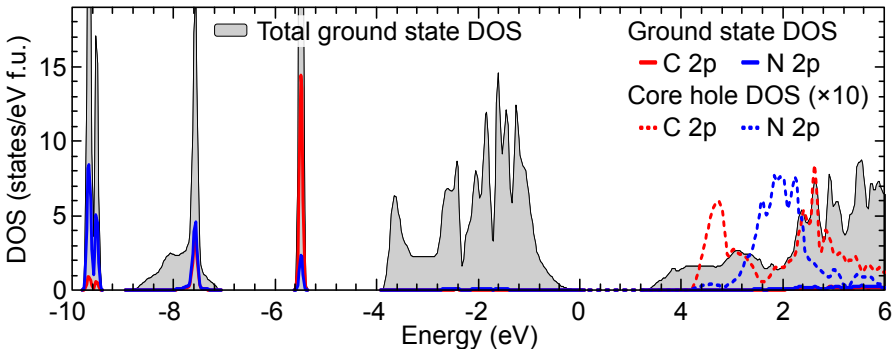

Figure S3: Calculated DOS of $MAPbI_3$ showing the total DOS and the $2p$ partial DOS of carbon and nitrogen.

Table S1: Relaxed atomic coordinates and muffin-tin radii for $MAPbI_3$. Lattice parameters are (a,b,c) = (6.22000238405, 6.22000238405, 6.22000238405) Å, and (α, β, γ) = (90.0°, 90.0°, 90.0°).

Atom	x	y	z	R_{MT}
Pb	0.045822	0.99995308	0.04403179	2.5
I	0.54511314	8.44e-06	0.07212391	2.5
I	0.01699702	0.49995815	0.06199484	2.5
I	0.04043888	2.292e-05	0.55003796	2.5
C	0.50448331	0.49999101	0.61645725	1.34
N	0.49891643	0.49999188	0.37704548	1.27
H	0.6727233	0.49999964	0.66925331	0.68
H	0.42131893	0.64474858	0.67335446	0.68
H	0.42130489	0.35523821	0.67333842	0.68
H	0.57267496	0.63533375	0.31262092	0.68
H	0.34143858	0.49998522	0.31855815	0.68
H	0.57265802	0.36464124	0.31260908	0.68

Table S2: Relaxed atomic coordinates and muffin-tin radii for a CH_3I-PbI_2 defect. Lattice parameters are (a,b,c) = (6.22000238405, 6.22000238405, 6.22000238405) Å, and (α, β, γ) = (90.0°, 90.0°, 90.0°).

Atom	x	y	z	R_{MT}
Pb	0.92755507	0.00044945	0.13701196	2.5
I	0.43012064	0.00013548	0.06706983	2.29
I	0.82643024	0.50037732	0.23115688	2.29
I	0.98464803	8.002e-05	0.63191284	2.29
C	0.56567357	0.50019912	0.46193214	1.33
H	0.64114054	0.50022864	0.62054735	0.72
H	0.47537241	0.64731656	0.4269946	0.72
H	0.47560537	0.3529286	0.42708629	0.72

Table S3: Relaxed atomic coordinates and muffin-tin radii for NH_3 within a PbI framework. Lattice parameters are (a,b,c) = (6.22000238405, 6.22000238405, 6.22000238405) Å, and (α, β, γ) = (90.0°, 90.0°, 90.0°).

Atom	x	y	z	R_{MT}
Pb	0.95173341	0.99871285	0.98904777	2.5
I	0.47750206	0.99775163	0.10531171	2.5
I	0.05188876	0.49889227	0.05453112	2.5
I	0.06088521	0.99903504	0.51071148	2.5
N	0.50851481	0.49649114	0.52084294	1.25
H	0.52320986	0.63122398	0.42770057	0.67
H	0.35943765	0.49833791	0.59016691	0.67
H	0.51702551	0.36557982	0.42160632	0.67

References

(1) Regier, T.; Krochak, J.; Sham, T.; Hu, Y.; Thompson, J.; Blyth, R. *Nucl. Instrum. Methods Phys. Res., Sect. A* **2007**, *582*, 93–95.

(2) Blaha, P.; Schwarz, K.; Madsen, G. K. H.; Kvasnicka, D.; Luitz, J. *WIEN2k, An Augmented Plane Wave + Local Orbitals Program for Calculating Crystal Properties*; Karlheinz Schwarz, Techn. Universität Wien, 2001.

(3) Perdew, J.; Burke, K.; Ernzerhof, M. *Phys. Rev. Lett.* **1996**, *77*, 3865–3868.

(4) Delugas, P.; Filippetti, A.; Mattoni, A. *Phys. Rev. B* **2015**, *92*, 045301.

(5) Marks, L. D. *J. Chem Theory Comput.* **2013**, *9*, 2786–2800.

(6) Neckel, A.; Schwarz, K.; Eibler, R.; Rastl, P.; Weinberger, P. *Microchim. Acta Suppl.* **1975**, *6*, 257.